Ultrasonics Sonochemistry 17 (2010) 427–434

Contents lists available at ScienceDirect

Ultrasonics Sonochemistry

journal homepage: www.elsevier.com/locate/ultsonch

Effect of ultrasound on the solubility limit of a sparingly soluble solid

D. Krishna Sandilya, A. Kannan *

Department of Chemical Engineering, Indian Institute of Technology Madras, Chennai 600036, Tamil Nadu, India

ARTICLE INFO

Article history:
Received 25 June 2009
Received in revised form 2 October 2009
Accepted 8 October 2009
Available online 13 October 2009

Keywords:
Ultrasound
Rate of attainment of saturation
Supersaturation
Temperature control
Volumetric mass transfer coefficient

ABSTRACT

The influence of power ultrasound (20 kHz) on the rate of attainment of saturation of sparingly soluble benzoic acid in distilled water and in 24% (w/w) aqueous glycerol was experimentally investigated at 30 °C. The importance of proper temperature control of process vessel contents when it was irradiated with high ultrasonic power level settings was demonstrated. A method was proposed to calculate the volumetric mass transfer coefficient under non-isothermal conditions.

1. Introduction

Solid dissolution and its subsequent dispersion in a solvent are of particular interest in several industrial situations. It finds widespread applications in multi-disciplinary fields such as mineral processing [1], chemical engineering [2,3], petroleum engineering [4] and nuclear engineering [5]. Specific examples of these include beneficiation of ores [6], extraction of perfumes from flowers [7], extraction of oils from seeds [8,9], extraction of useful medicinal products from natural materials [10–12], electrochemistry [13], acid leaching [14–20], dissolution of pharmaceutical compounds [21], dissolution of non-volatile explosives in groundwater [22], dissolution of scales formed by mineral deposits in petroleum pipelines [4] and dissolution of plutonium oxide (PuO_2), an important step in the preparation of nuclear fuels [5].

The basic rate limiting issue viz. resistance to mass transfer is common to all these applications. It is difficult to dissolve sparingly soluble solids in a solvent even when they are dispersed as fine particles. The dissolution rate of a solute in a solvent is a function of its saturation limit in that solvent, state of aggregation, prevailing hydrodynamics created by the mixing device used, temperature and solvent characteristics. It is necessary to design innovative devices in which solid dissolution processes may be intensified.

Acoustic cavitation induced through ultrasound (US), sound of frequency greater than 20 kHz, has several multi-disciplinary applications. Previous studies have shown that ultrasound has a great potential in intensifying the rates and altering the pathways of chemical reactions [23]. While the focus has been on intensifying rates and altering chemical reaction pathways through ultrasound, relative less focus has been given to its physical effects. While ultrasound has been routinely used in industries for cleaning purposes, opportunities exist for extending its application to several processes in chemical engineering limited by mass transfer. While several studies exist on intensifying gas–liquid mass transfer in literature, the enhancement of solid–liquid mass transfer has scantily been reported. The mass transfer associated with the batch dissolution of a sparingly soluble solute in a solvent is given by the following equation:

$$\frac{dC}{dt} = k_c\left(\frac{S}{V}\right)(C^* - C) \tag{1}$$

This equation may be integrated and the plot of $-\ln(1 - C/C^*)$ versus time will yield a straight line, the slope of which is the volumetric mass transfer coefficient (k_ca). It is well established that the intrinsic mass transfer coefficient (k_c), and the specific interfacial area (S/V) are enhanced by microstreaming and microjets, respectively, in an acoustic field [23]. When a solid–liquid system in which solids are dispersed as particles is exposed to ultrasound, the solid particles get fragmented by the microjets that are created by the acoustic field. This fact could be exploited to enhance mass transfer rates since the interfacial area available for the transport process increases in the presence of ultrasound. On the other hand, to the best of our knowledge, only one study [24] had been reported which delineates the effect of ultrasonic irradiation on the saturation limit (C^*) in a solid–liquid system. They considered two solid–liquid systems (sodium sulfide in acetonitrile and calcium citrate in water)

* Corresponding author. Tel.: +91 44 2257 4170; fax: +91 44 2257 4152.
E-mail address: kannan@iitm.ac.in (A. Kannan).

1350-4177/$ - see front matter © 2009 Elsevier B.V. All rights reserved.
doi:10.1016/j.ultsonch.2009.10.005

Nomenclature

a	interfacial area, m^2/m^3
C	concentration of solute in aqueous solution, mol/m^3
$C_{t=0}$	concentration of solute in aqueous solution at time $t = 0$, mol/m^3
C_t	concentration of solute in aqueous solution at any time t, mol/m^3
C^*	saturation limit of sparingly soluble solute, mol/m^3
C^*_{30}	saturation limit of sparingly soluble solute at 30 °C, mol/m^3
C^*_{30G}	saturation limit of sparingly soluble solute in 24% (w/w) aqueous glycerol at 30 °C, mol/m^3
C^*_{30W}	saturation limit of sparingly soluble solute in distilled water at 30 °C, mol/m^3
C^*_{ref}	saturation limit of sparingly soluble solute at reference temperature T_{ref}, mol/m^3
C^*_T	saturation limit of sparingly soluble solute at a temperature T, mol/m^3
k_c	intrinsic mass transfer coefficient, m/s
k_ca	volumetric mass transfer coefficient, s^{-1}
m	temperature pre-exponent in Eq. (4), K^{-1}
S	surface area, m^2
t	time, s
T	temperature, °C/K
V	volume of solvent, m^3

Acronym

US	ultrasound

and concluded that ultrasound had enhanced the saturation limit by inducing supersaturation in the system. The level of supersaturation (C/C^*) was reported to be 1.4 and 1.7 for sodium sulfide–acetonitrile and calcium citrate–water, respectively. Kannan and Pathan [25] observed a nearly fivefold enhancement in intrinsic mass transfer coefficient (k_c) used in Eq. (1) when dissolving the sparingly soluble cylinder made of benzoic acid in water when ultrasound was applied at 20 kHz frequency.

Based on the above it may be observed that solid dissolution in the presence of ultrasound is governed by enhancement in volumetric mass transfer coefficient and also by the phenomenon of supersaturation. It has to be seen whether supersaturation is also significant for the benzoic acid model test system used in this work. The objectives of the current work hence are

(a) Study the effect of ultrasound on the rate of attainment of saturation limit (C^*) of the sparingly soluble benzoic acid in two solvents viz. distilled water and 24% (w/w) aqueous glycerol.
(b) Estimate the volumetric mass transfer coefficient (k_ca) at different power levels of ultrasound.

2. Experimental details

2.1. Materials

Sparingly soluble benzoic acid was chosen as the solute in this study. Benzoic acid particles as received from HiMedia, Mumbai (AR grade) were sieved to give an average feed particle size of 1800 μm (size range of sieves: −2 + 1.6 mm; DIN standards) in all the runs. The solvent was either distilled water or 24% (w/w) aqueous glycerol solution. AR grade glycerol (Ranbaxy Fine Chemicals Ltd., New Delhi) and distilled water were used to prepare 24% (w/w) aqueous glycerol solution. The physical properties of solvents at 30 °C are given in Table 1.

2.2. Experimental setup

Saturation limit studies were carried out in a jacketed cylindrical vessel, which was made of either perspex or stainless steel (Fig. 1). A cryostat (Ultra Cryostat Circulator, Scientific Instruments, Chennai) was used to maintain constant temperature. An ultrasonic probe (model VCX-500, Sonics and Materials Inc., USA), rated at 500 W with a resonating frequency of 20 kHz and a tip diameter of 13 mm was used to induce ultrasonic waves in the process vessel. Various levels of ultrasonic power input, expressed as a percentage of maximum setting, were used either in continuous or intermittent mode. The ultrasonic power level setting was applied in the continuous mode between 30% and 70% (both settings inclusive) of maximum in increments of 10%. In the intermittent mode of operation, the instrument power setting was fixed at 70% and operated with sonication for 5 s alternating with absence of sonication for the same interval of time. The time of sonication varied between 30 and 240 min depending on the power setting. For example, in case of a run with 70% ultrasonic power level setting, the process time was set to 30 min as against 240 min for 30% power level setting case. The actual power dissipated in the liquid as a function of percentage setting was obtained from calorimetry studies [26] and reported in Section 2.4.

2.3. Experimental procedure

The saturation limit of benzoic acid in each solvent, in the absence of ultrasound, was measured experimentally at 30 °C. Excess amount of solute (10 g) was taken in a vessel containing one liter of solvent and the contents were mechanically stirred for several hours. The temperature of the vessel contents was maintained at 30 ± 0.5 °C using a cryostat. The concentration of benzoic acid was monitored at regular intervals of time. The experiment was carried out till a plateau was obtained in the concentration versus time plot. The saturation limit values of benzoic acid in both the solvents at 30 °C are given in Table 1. The solubility of benzoic acid in water is available in literature [27,28] and the presently reported value is in agreement within 0.5%. However, data for solubility of benzoic acid in aqueous glycerol solution are mainly reported in literature at 25 °C whereas in the present work the solubility value is reported for experimental conditions at 30 °C.

In a typical run carried out in the presence of ultrasound, 10 g of benzoic acid particles was charged into the process vessel containing 800 mL of solvent. The ultrasound probe was positioned at the centre of the vessel. The ultrasonic generator was then switched on after setting the power to the desired level. Cooling water was circulated in the jacket to maintain the temperature inside the process vessel at 30 °C. The temperature of process vessel contents was monitored at regular intervals of time with a digital thermometer (model ST-9263A/B/C, Yi Chun Electrics Co. Ltd., Taiwan) which has a resolution of ±0.1 °C. The digital thermometer was immersed directly in the process solution. The sensing time of digital thermometer used

Table 1
Physical properties of solvents (at 30 °C) used in present study.

Item number	Solvent	Saturation limit of benzoic acid (kg/m^3)	Density (kg/m^3)	Viscosity (cP)	Heat capacity (J/kg °C)
1	Distilled water	4.04	996	0.85	4184
2	24% (w/w) Aqueous glycerol	4.44	1054	1.76	3789

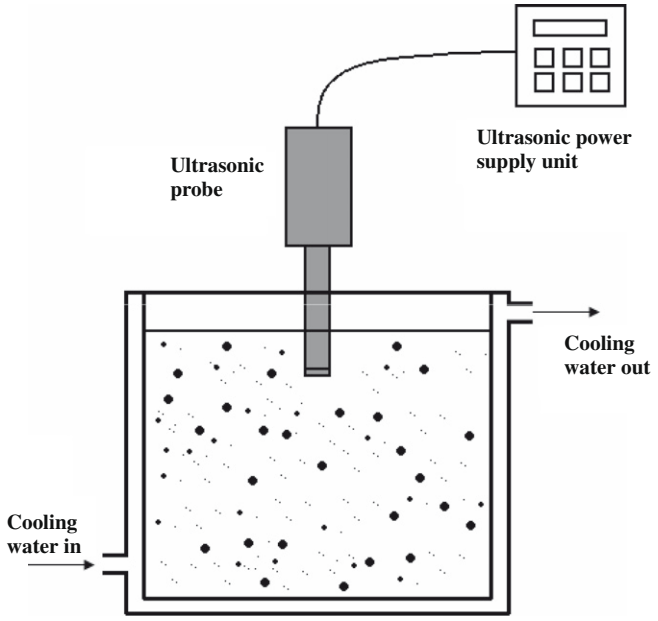

Fig. 1. Schematic of experimental setup for saturation limit studies.

was one second. Samples for concentration analysis were withdrawn at regular intervals of time using a syringe-driven filter. The reproducibility of experimental results was within ±2%.

The volumetric mass transfer coefficients were estimated from the initial rates for sonicated conditions after integration of Eq. (1). The plot of $\ln\left(\frac{C^* - C_{t=0}}{C^* - C_t}\right)$ versus time will yield a line slope of $k_c \frac{S}{V}$. Since either pure distilled water or 24% (w/w) aqueous glycerol solution was taken at the beginning of each run without any benzoic acid solute, $C_{t=0}$ is equal to zero.

The samples taken out at different times were diluted to the required extent and analyzed using a UV–vis spectrophotometer (model V-530, JASCO, Japan) by recording the absorbance value at 227 nm for benzoic acid in distilled water and at 228 nm for benzoic acid in 24% (w/w) aqueous glycerol. Some analyses were also carried out using titration with 0.01 N NaOH. There was not much variation between the two analytical techniques. The viscosity of each solvent was determined using the Rheometer (Physica MCR 301, Anton Paar GmbH, Germany) in the High Polymer Engineering Laboratory, IIT Madras. The particle size distributions at each experimental combination of ultrasonic power level setting and sonication time were measured in a laser particle size analyzer (S3500, Microtrac Inc., USA), which has a measuring range from 0.025 to 1408 μm.

2.4. Calorimetry

The amount of power absorbed by each solid–liquid system was measured using calorimetry [26]. The power dissipated in stainless steel (SS) vessel for each solid–liquid system is shown in Table 2. It is to be noted that the power dissipation studies are actually based on experiments carried out in the presence of particles.

3. Results and discussion

3.1. Effect of temperature on saturation limit

3.1.1. Studies in perspex vessel

Initially, the experiments on the rate of attainment of saturation were conducted in a process vessel made of perspex. Fig. 2 compares the effect of continuous sonication at 30% and 70% power level settings on the rate of attainment of saturation limit of benzoic acid in distilled water. Even though oscillatory behaviour was evident in the dissolved concentration between 30 and 180 min of 30% sonication, the concentration eventually reached the saturation value after 210 min (3.5 h). Further sampling after 240 min of sonication did not indicate any supersaturation in the system. The circulating water bath ensured that the temperature rise did not exceed 1.5 °C. It has to be noted that the solids were not properly mixed at 30% ultrasonic power level setting. Fig. 3 depicts the mixing induced by ultrasound (at 30% and 70% power level settings) for benzoic acid–distilled water system. For the sake of visual observation, these photographs were taken with particles suspended in a 1 L glass beaker. Particles had a tendency to form agglomerates at 30% ultrasonic power level setting (Fig. 3ii) and hence the effective area available for mass transfer was not enhanced. So, the system attained saturation limit only after 3.5 h of sonication at 30% power level setting and the system did not get supersaturated in the 4-h run. The microstreaming action of ultrasound may have caused the dissolution even though there was no appreciable physical bulk movement (mixing) of particles. The shock waves produced as a result of collapse of cavitation bubbles induce a microscopic turbulence around the solid particles and hence reduce the film surrounding the solid particle [23].

Fig. 2 also shows the rate of dissolution of benzoic acid in distilled water in presence of ultrasound at 70% power level setting. Vigorous mixing of particles was now observed (Fig. 3iii). The particles were well suspended and eventually finely dispersed after 5 min of sonication at 70% power level setting (Fig. 3iv). The system has reached the saturation concentration only after about 9 min of sonication. Ultrasound could accelerate the rate of attainment of saturation rapidly. In the case of 70% power level setting, a slight supersaturation was observed for sometime in the system (1.03 times the saturation concentration obtained by mechanical stirring), as is evident from Fig. 2. Instantaneous temperature control was difficult under continuous sonication at this power input (4 °C rise was observed for sometime even though ice was added in the circulating water bath). The collapse of cavitation bubbles will be more violent at 70% power level setting compared to that

Table 2
Power dissipated in stainless steel vessel for different systems of present study.

Solvent	Ultrasonic power level setting (% of maximum)	Specific power dissipation (W/L)
Distilled water	30	43.4
	50	68.5
	70	115.1
24% (w/w) Aqueous glycerol	30	41.8
	50	77.9
	70	114.5

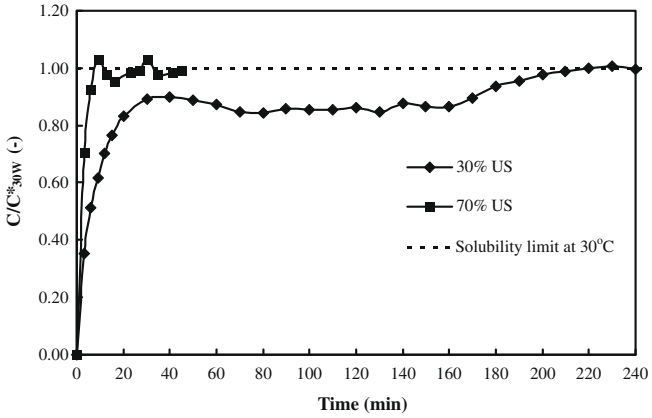

Fig. 2. Rate of attainment of saturation concentration in presence of ultrasound (30% and 70% power level settings) for benzoic acid–distilled water at 30 °C in perspex vessel.

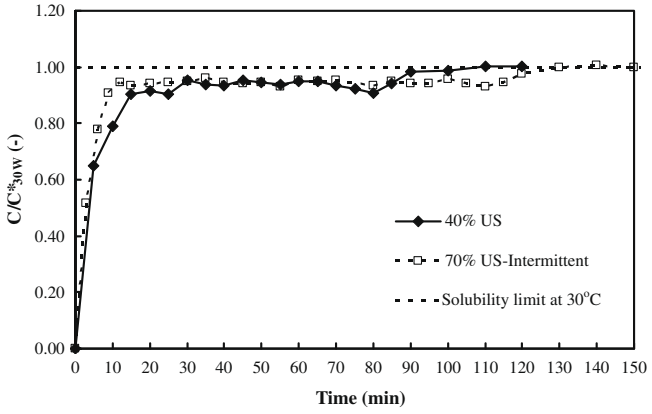

Fig. 4. Rate of attainment of saturation concentration under different methods of sonication for benzoic acid–distilled water system at 30 °C in perspex vessel.

at 30% power level setting. When cavitation bubbles collapse in the vicinity of solid particles, microjets will form and hit the surface of solid particles perpendicularly [23] with great speed estimated at 100 m/s [29]. This leads to pitting and erosion of solid particles which improves the surface area available for mass transfer [23].

Hence it was decided to opt for the intermittent mode of sonication (5 s of ultrasonic excitation and an immediate shut off for the next 5 s) over a longer duration at the higher power setting. Fig. 4 shows that the concentration trends of runs with 70% intermittent sonication and 40% continuous sonication for benzoic acid–distilled water are comparable at almost all the sampled times until 90 min of operation. The power dissipated in the system under 70% intermittent sonication (73.91 W) was almost double than that for 40% continuous sonication (37.5 W). During the intermittent pause in sonication, the particles were observed to completely settle to the base of the vessel within 2–3 s. Hence even though 70% intermittent sonication does have higher power dissipation, it is only as effective as 40% continuous ultrasound. The intermittent mode of operation enabled better temperature control at the highest input level (70%) as there was sufficient time for the system to get cooled between each ultrasonic excitation.

Fig. 5 depicts the concentration of benzoic acid in a viscous solvent viz. 24% (w/w) aqueous glycerol as a function of time at different ultrasonic power inputs. In contrast to the previous case involving distilled water (Fig. 2), there were no frequent oscillations in the concentration values for this system. Instantaneous

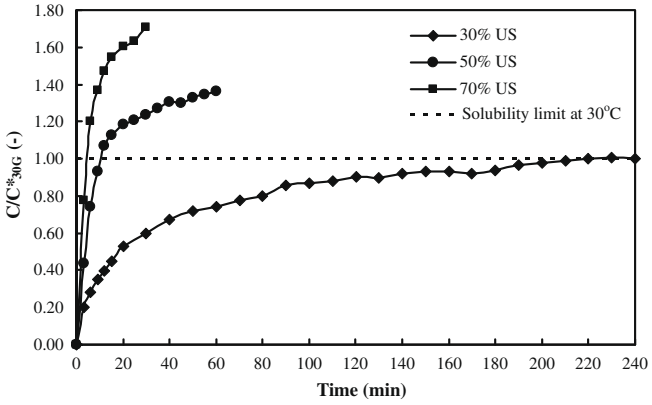

Fig. 5. Rate of attainment of saturation concentration in presence of ultrasound for benzoic acid–24% (w/w) aqueous glycerol in perspex vessel.

temperature control in the perspex vessel was more difficult in the benzoic acid–24% (w/w) aqueous glycerol system than in the benzoic acid–distilled water system owing to the higher viscosity of the former system (Table 1). At moderate ultrasound power levels, temperature control was not an issue and even the benzoic acid–24% (w/w) aqueous glycerol system reached saturation without any oscillations. When the temperature rose rapidly in the benzoic acid–24% (w/w) aqueous glycerol system due to insufficient

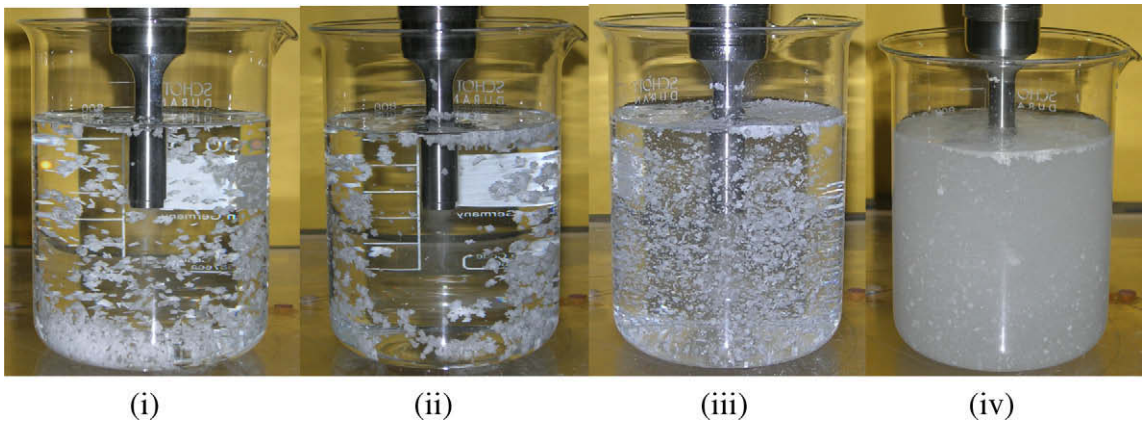

Fig. 3. Visualization of mixing of benzoic acid particles in water at different ultrasonic power level settings and sonication times: (i) 30% US after 30 s, (ii) 30% US after 5 min, (iii) 70% US after 30 s and (iv) 70% US after 5 min.

cooling in the perspex container, solubility increased rapidly. Hence, the solute dissolved at a much faster rate and to a greater extent in the liquid so that concentration oscillations were not present. At higher power levels, the temperature rise could be minimized with difficulty in the benzoic acid–distilled water case, and fluctuations were observed. These in turn were reflected in the concentration fluctuations in the benzoic acid–distilled water system.

It could be observed from Fig. 5 that there seems to be a significant supersaturation in the runs involving glycerol system at the power level settings of 50% and 70%. The scaled level of supersaturation with respect to silent run saturation value (C/C^*_{30G}) induced in the system at these conditions was 1.36 and 1.71, respectively. However, there was also a substantial rise in temperature from the starting value of 30 °C in both the cases, viz. 6 °C at 50% power level setting and 12 °C at 70% power level setting (Fig. 6), which may have enhanced the saturation limits.

To estimate the primary effect of temperature on saturation limit, separate studies were conducted in a constant temperature bath in which the saturation limits of benzoic acid in 24% (w/w) aqueous glycerol between 30 and 50 °C were measured. The saturation limits of benzoic acid in 24% (w/w) aqueous glycerol at different temperatures thus obtained were found to follow a linear trend in this range of temperature:

$$\frac{C^*_T}{C^*_{30G}} = 1 + 0.0718(T - 303) \quad (2)$$

where T is in Kelvin and C^*_{30G} is the saturation concentration of benzoic acid in 24% (w/w) aqueous glycerol at 30 °C. The R^2 for this fit was 0.9980.

From Eq. (2), the expected values of C/C^*_{30G} have been calculated according to the prevailing temperature at a particular time instant. They were found to be in good agreement with those measured experimentally (within ±5%) as shown in Fig. 7 for 50% and 70% power level settings. Hence it may be concluded that the supersaturation observed in 50% and 70% power level setting cases ($C/C^*_{30G} = 1.36$ and $C/C^*_{30G} = 1.71$, respectively) for benzoic acid–24% (w/w) aqueous glycerol system was not due to an unexpected effect of ultrasonic irradiation; rather, it was an apparent supersaturation attained by the solid–liquid system as a result of temperature rise inherent in ultrasonic operation especially at higher power level settings.

In light of the above discussion, it is important to perform the saturation limit experiments with more accurate temperature control. In order to control the temperature inside the process vessel accurately at 30 ± 2 °C, at all the power level settings of ultrasonic irradiation, a stainless steel process vessel was fabricated and used in further experimentation.

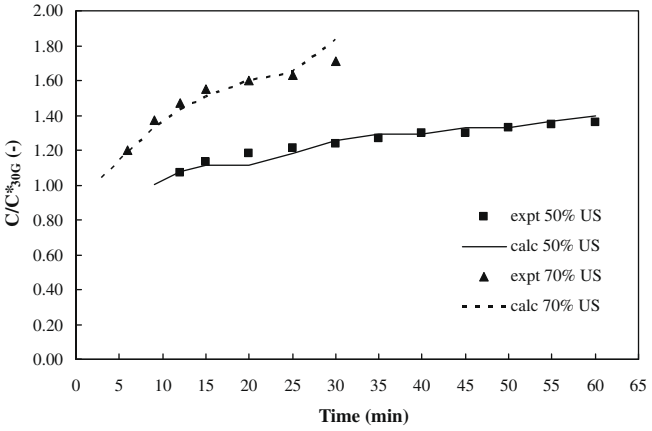

Fig. 7. Comparison of calculated and experimental C/C^*_{30} for benzoic acid–24% (w/w) aqueous glycerol system at 50% and 70% ultrasonic power level settings in perspex vessel.

3.1.2. Studies in stainless steel vessel

Solubility limit experiments in presence of ultrasound with good temperature control (30 ± 2 °C) were carried out in a stainless steel vessel. This vessel has the same dimensions as those of perspex one. As shown in Fig. 8, there was no supersaturation in presence of ultrasound at a power level setting of 60% for benzoic acid–24% (w/w) aqueous glycerol (70% US in perspex vessel and 60% US in stainless steel vessel correspond to comparable specific power input). Also, the temperature control was very good during the run (30 ± 1 °C). The system had just reached saturation concentration in 15 min and did not exceed the saturation limit significantly during the 45-min run. Fig. 8 also shows the rate of attainment of saturation for benzoic acid–distilled water system at 70% power level setting. The temperature control was very good (30 ± 1 °C) during the 45-min run and the system had attained saturation concentration in 12 min. The oscillations that were present in the distilled water system when experiments were carried out in a perspex vessel (Fig. 2) were absent when the stainless steel vessel was used (Fig. 8).

3.2. Absence of supersaturation in the present solid–liquid systems

Thompson and Doraiswamy [24] observed significant supersaturation (of the order of 1.4 times the saturation concentration) in

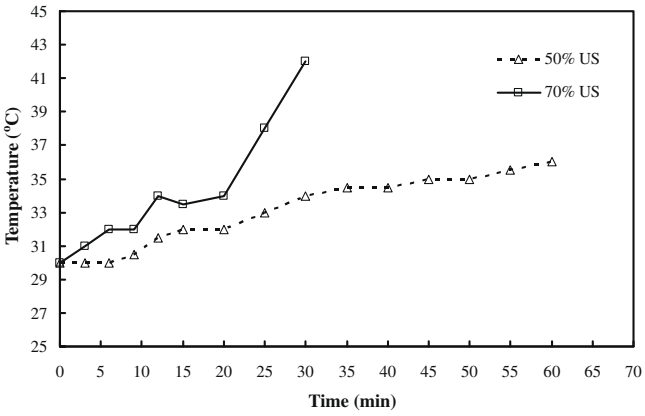

Fig. 6. Temperature rise in presence of ultrasound (50% and 70% power level settings) for benzoic acid–24% (w/w) aqueous glycerol in perspex vessel.

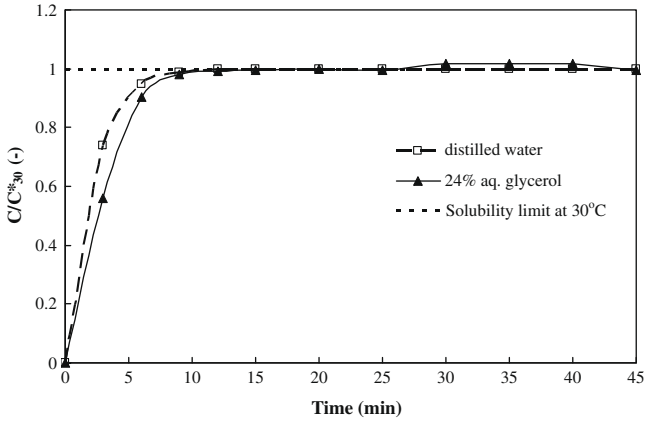

Fig. 8. Rate of attainment of saturation concentration in presence of ultrasound in stainless steel vessel.

their ultrasonic dissolution of sodium sulfide in acetonitrile solvent. The power absorbed by their system was 95.4 W whereas that entering the system, as quoted by manufacturer, was 166 W [24]. The power absorbed by the system per unit volume was 2385 W/L in their study. However, in the present study, no supersaturation was observed in the present run. At the maximum 70% power setting, the power dissipated per unit volume was 115 W/L.

The supersaturation reported by Thompson and Doraiswamy [24] was attributed to (i) the existence of SCF (supercritical fluid) conditions as a result of the implosion of acoustic bubble and (ii) Ostwald ripening owing to presence of the very small particles (<1.0 μm). It has to be noted that the average feed particle size was ~34 μm in the study of Thompson and Doraiswamy [24] and hence ultrasound might have generated very small particles as a result of its comminution ability. But in the current investigation, we used an average feed particle size of 1800 μm in all the batches. The average particle size attained for benzoic acid–distilled water system at the highest power level setting used (70%) and 30 min of continuous sonication was 47.16 μm. In addition to that, the volume of the solid–liquid system studied by Thompson and Doraiswamy [24] was not mentioned in their paper whereas that of the present investigation was 800 mL. But the schematic of the experimental apparatus shown in this paper [24] is the same as that presented in a previous paper of Hagenson and Doraiswamy [26] wherein the details of experimental apparatus are given. So, it was assumed that the volume of solid–liquid system used in the work of Thompson and Doraiswamy [24] was 40 mL. The suspension density (weight of solute/volume of solvent) in their work was 100 g/L (4 g of solute in 40 mL of solvent) whereas it was 12.5 g/L (10 g of solute in 800 mL of solvent) in the present study. The small average feed particle size (~34 μm) in their work may have contributed towards the attainment of supersaturation in presence of ultrasound. The particle size reduction in presence of ultrasound depends on the characteristics of solid, physical properties of solvent and the intensity of ultrasound prevailing in the solid–liquid system [23].

A separate set of experiments was carried out to observe the effect of smaller average feed particle size and higher suspension density. A particle feed size of 58 μm and suspension density of 50 g/L (2 g of solute in 40 mL of solvent) were taken and the ultrasound power setting was fixed at 70% power level. Temperature of vessel contents was maintained at 30 ± 1 °C. The concentration trends of benzoic acid–distilled water and benzoic acid–24% (w/w) aqueous glycerol systems obtained under these conditions are shown in Fig. 9. It is interesting to note that both the systems have shown almost the same behaviour in terms of rate of attainment of saturation despite a twofold difference in viscosity. There was no supersaturation in both the systems and the average particle size was reduced to 39 μm after 45 min of sonication. A minor volume fraction of very small particles with diameter less than 1.0 μm (0.55%) was observed in the run with distilled water but no particles were present in this size range in the run with 24% (w/w) aqueous glycerol. However, the volume fraction of particles in the size range 1.0–10.0 μm was somewhat higher (11% by weight for run with distilled water and 3% for run with 24% (w/w) aqueous glycerol) in the particle size distribution after 45 min of sonication in both the systems. The mass fraction of particles of diameter less than 1.0 μm may have been higher in Thompson and Doraiswamy [24] work and this may have driven the system towards supersaturation. It was expected that a larger starting particle size (58 μm) and smaller suspension density (50 g/L) when compared to Thompson and Doraiswamy [24] may have facilitated more intense particle breakage by ultrasound leading to supersaturation. However, this was not the case in view of the present results. It appears that the supersaturation in a solid–liquid system induced by ultrasound is not a general phenomenon and depends on several factors such as solid characteristics, solvent properties, ultrasound intensity as well as extent of temperature control in the process vessel. Further investigations are essential to delineate the mechanistic features of ultrasound-assisted solid dissolution.

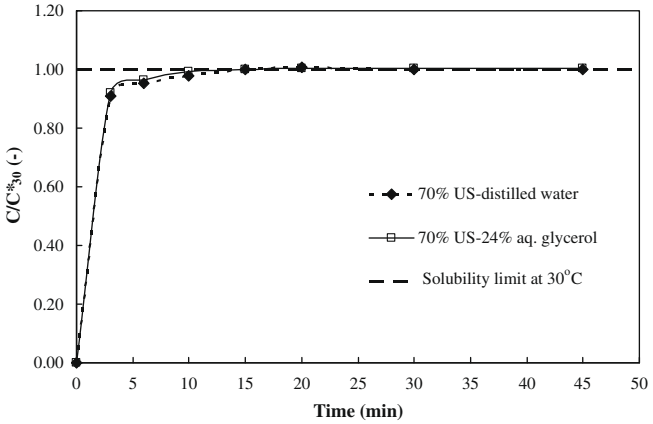

Fig. 9. Rate of attainment of saturation concentration in presence of ultrasound (70% power level setting) with smaller feed size particles. (Here concentrations are normalized by the respective C* values at 30 °C for aqueous glycerol solution and distilled water.)

3.3. Estimation of volumetric mass transfer coefficients

3.3.1. Isothermal conditions

Under isothermal conditions, Eq. (1) can be integrated and the volumetric mass transfer coefficient can be determined as outlined in Section 2.3. In this work, the volumetric mass transfer coefficient $k_c a$ values are reported under isothermal conditions only.

3.3.2. Non-isothermal conditions

In the case where the temperature rises during the dissolution process as shown in Fig. 6 the volumetric mass transfer coefficient may be calculated as follows.

Let the temperature dependency of volumetric mass transfer coefficient be modeled according to

$$k_c a = k_c a(T) \tag{3}$$

For moderate temperature rises, a linear relation may be considered as follows:

$$k_c a = (k_c a)_0[1 + m\Delta T] \tag{4}$$

where

$$\Delta T = T - T_{ref} \tag{5}$$

Here T_{ref} is the reference temperature that is also be the temperature at the start of the experiment (time $t = 0$). In an isothermal operation, T_{ref} is the set point temperature that needs to be maintained a constant. The actual temperature is given by T and $(k_c a)_0$ is the volumetric mass transfer coefficient under isothermal conditions. From measurements, if the variation of temperature with time is known, the volumetric mass transfer coefficient for the non-isothermal operation may be estimated by numerically solving the following system of equations:

$$V\frac{dC}{dt} = (k_c a)_0[1 + m\Delta T](C^* - C) \tag{6}$$

where

$$\frac{C^*}{C^*_{ref}} = 1 + q(\Delta T) \tag{7}$$

$$T = T(t) \tag{8}$$

This procedure is demonstrated for the case illustrated in Fig. 6. In the experiment involving 50% power level setting, the temperature control for the benzoic acid–24% (w/w) aqueous glycerol system could not be maintained constant and it's variation with time was expressed as

$$\Delta T = T - 303.15 = 7.14\left\{1 - \exp\left[-\frac{(t-6)}{32.49}\right]\right\} \tag{9}$$

This equation shows that there was a dead time of six minutes before the temperature rise occurred. Eq. (9) was substituted in Eqs. (4) and (5). The resulting expressions were used in Eq. (6) and numerical integration was carried out using ODE45 routine of MATLAB® (The MathWorks Inc.). Here the unknown parameters $(k_c a)_0$ and m were estimated using the experimental data for concentration of benzoic acid in the glycerol system (Fig. 5) obtained under the non-isothermal conditions. The parameter estimation was carried out simultaneously with numerical integration of Eq. (6) using the FMINS routine in MATLAB®. The parameters were obtained by minimizing the square of the deviations of the numerical predictions from the experimental data. The estimated parameters are given below and the resulting fit is also shown in Fig. 10:

$$(k_c a)_0 = 3.5 \times 10^{-3}\ \mathrm{s}^{-1}$$

$$m = 2.79\ \mathrm{K}^{-1}$$

Hence the above procedure may be adopted for non-isothermal operation once the variation of temperature with time is known during the course of the run. It is clear that the increase in concentration with time is also due to the increase in the concentration driving force with time which in turn is caused by increase in C^* with temperature (Eq. (7)). Further the volumetric mass transfer coefficient rise with temperature is also separately accounted for in Eq. (4) thereby delineating the effects of temperature on the volumetric mass transfer coefficient and the concentration driving force. Another precaution to note is that a linear variation in temperature with time may not be generally assumed during the course of the experimental run when the temperature rise is significant.

3.3.3. Comparison of isothermal $k_c a$ values at different power levels

Fig. 11 shows the comparison of volumetric mass transfer coefficients obtained for benzoic acid–distilled water and benzoic acid–24% (w/w) aqueous glycerol systems at different ultrasonic power level settings. The volumetric mass transfer coefficient obtained for benzoic acid–distilled water at 30% and 70% power level settings

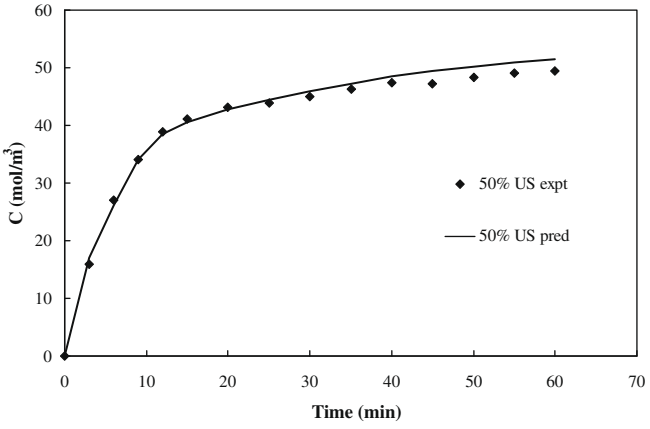

Fig. 10. Variation of concentration with time in the non-isothermal mass transfer study (50% power level setting, benzoic acid–24% (w/w) aqueous glycerol system).

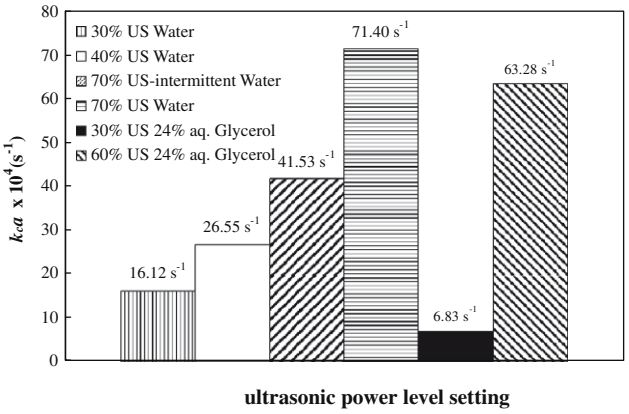

Fig. 11. Comparison of volumetric mass transfer coefficients under ultrasonic conditions for benzoic acid–distilled water and benzoic acid–24% (w/w) aqueous glycerol.

for this system were 1.61×10^{-3} and $7.14 \times 10^{-3}\ \mathrm{s}^{-1}$, respectively. This clearly shows an enhancement factor of 4.4 with 70% power level setting when compared to 30% power level setting. A ninefold increase in volumetric mass transfer coefficient was observed for benzoic acid–24% (w/w) aqueous glycerol system with 60% power level setting when compared to that obtained by 30% power level setting.

4. Conclusions

Ultrasound had increased the rate of attainment of saturation limit rapidly in both the solid–liquid systems studied. Nevertheless, it did not induce any supersaturation in the two solid–liquid systems for the process conditions studied. Proper temperature control of process vessel contents is essential while treating them with ultrasound at higher power level settings. The volumetric mass transfer coefficient in presence of ultrasound was found to increase with increase in ultrasonic power level setting for both the systems studied. When the experiments are carried out under conditions where the temperature increases due to sonication, the increase in the saturation concentration (C^*) must also be accounted for in the volumetric mass transfer coefficient estimation.

Acknowledgements

The authors are grateful to Prof. Paramanand Singh, IIT Madras for providing the particle size analyzer facility. We also thank Mr. M. Subramanian, IIT Madras for assisting in photography.

References

[1] H. Özbek, Y. Abali, S. Çolak, I. Ceyhun, Z. Karagölge, Dissolution kinetics of magnesite mineral in water saturated by chlorine gas, Hydrometallurgy 51 (1999) 173–185.
[2] J.A.R. Bennett, J.B. Lewis, Dissolution rates of solids in mercury and aqueous liquids: the development of a new type of rotating dissolution cell, AIChE Journal 4 (1958) 418–422.
[3] M. Wallin, I. Bjerle, A mass transfer model for limestone dissolution from a rotating cylinder, Chemical Engineering Science 44 (1989) 61–67.
[4] G.P.P. Gunarathne, R.W. Keatch, Novel techniques for monitoring and enhancing dissolution of mineral deposits in petroleum pipelines, Ultrasonics 34 (1996) 411–419.
[5] F. Juillet, J.M. Adnet, M. Gasgnier, Ultrasound effects on the dissolution of refractory oxides (CeO_2 and PuO_2) in nitric acid, Journal of Radioanalytical and Nuclear Chemistry 224 (1997) 137–143.
[6] A.K. Mesci, F. Sevim, Dissolution of magnesia in aqueous carbon dioxide by ultrasound, International Journal of Mineral Processing 79 (2006) 83–88.
[7] M. Romdhane, C. Gourdon, Investigation in solid–liquid extraction: influence of ultrasound, Chemical Engineering Journal 87 (2002) 11–19.

[8] H. Li, L. Pordesimo, J. Weiss, High intensity ultrasound-assisted extraction of oil from soybeans, Food Research International 37 (2004) 731–738.
[9] I.T. Stanisavljević, M.L. Lazić, V.B. Veljković, Ultrasonic extraction of oil from tobacco (*Nicotiana tabacum* L.) seeds, Ultrasonics Sonochemistry 14 (2007) 646–652.
[10] K.J. Lee, K.H. Row, Enhanced extraction of isoflavones from Korean soybean by ultrasonic wave, Korean Journal of Chemical Engineering 23 (2006) 779–783.
[11] J.-B. Ji, X.-H. Lu, M.-Q. Cai, Z.-C. Xu, Improvement of leaching process of Geniposide with ultrasound, Ultrasonics Sonochemistry 13 (2006) 455–462.
[12] X.U. Huaneng, Z. Yingxin, H.E. Chaohong, Ultrasonically assisted extraction of isoflavones from stem of *Pueraria lobata* (Willd.) Ohwi and its mathematical model, Chinese Journal of Chemical Engineering 15 (2007) 861–867.
[13] D.R. Gabe, D.J. Robinson, Mass transfer in a rotating cylinder cell – I. Laminar flow, Electrochimica Acta 17 (1972) 1121–1127.
[14] T. Tekin, D. Tekin, M. Bayramoglu, Effect of ultrasound on the dissolution kinetics of phosphate rock in HNO_3, Ultrasonics Sonochemistry 8 (2001) 373–377.
[15] H. Okur, T. Tekin, A.K. Ozer, M. Bayramoglu, Effect of ultrasound on the dissolution of colemanite in H_2SO_4, Hydrometallurgy 67 (2002) 79–86.
[16] T. Tekin, Use of ultrasound in the dissolution kinetics of phosphate rock in HCl, Hydrometallurgy 64 (2002) 187–192.
[17] Y. Tanaka, Q. Zhang, F. Saito, Sonochemical recovery of metals from recording media, Journal of Chemical Engineering of Japan 35 (2002) 173–177.
[18] H.T. Dogan, A. Kurtbas, T. Tekin, The effect of ultrasound on the dissolution of pyrite ores in acidic and $Fe_2(SO_4)_3$ solutions, Chemical Engineering and Technology 27 (2004) 87–89.
[19] H. Grénman, E. Murzina, M. Rönnholm, K. Eränen, J.-P. Mikkola, M. Lahtinen, T. Salmi, D.Y. Murzin, Enhancement of solid dissolution by ultrasound, Chemical Engineering and Processing 46 (2007) 862–869.
[20] S. Sakultung, K. Pruksathorn, M. Hunsom, Simultaneous recovery of valuable metals from spent mobile phone battery by an acid leaching process, Korean Journal of Chemical Engineering 24 (2007) 272–277.
[21] D. Mangin, E. Garcia, S. Gerard, C. Hoff, J.P. Klein, S. Veesler, Modeling of the dissolution of a pharmaceutical compound, Journal of Crystal Growth 286 (2006) 121–125.
[22] P.C. Gilcrease, V.G. Murphy, K.F. Reardon, Simultaneous grinding and dissolution of TNT solids in an agitated slurry, AIChE Journal 47 (2001) 572–581.
[23] L.H. Thompson, L.K. Doraiswamy, Sonochemistry: science and engineering, Industrial and Engineering Chemistry Research 38 (1999) 1215–1249.
[24] L.H. Thompson, L.K. Doraiswamy, The rate enhancing effect of ultrasound by inducing supersaturation in a solid–liquid system, Chemical Engineering Science 55 (2000) 3085–3090.
[25] A. Kannan, S.K. Pathan, Enhancement of solid dissolution process, Chemical Engineering Journal 102 (2004) 45–49.
[26] L.C. Hagenson, L.K. Doraiswamy, Comparison of the effects of ultrasound and mechanical agitation on a reacting solid–liquid system, Chemical Engineering Science 53 (1998) 131–148.
[27] A. Seidell, Solubilities of Inorganic and Organic Substances, D. Van Nostrand, New York, 1917.
[28] H. Sahay, S. Kumar, S.N. Upadhyay, Y.D. Upadhya, Solubility of benzoic acid in aqueous polymeric solutions, Journal of Chemical and Engineering Data 26 (1981) 181–183.
[29] K.S. Suslick, S.J. Doktycz, E.B. Flint, On the origin of sonoluminescence and sonochemistry, Ultrasonics 28 (1990) 280–290.